

Accepted Manuscript

Title: NtZIP11, a new Zn transporter specifically upregulated in tobacco leaves by toxic Zn level

Authors: Katarzyna Kozak, Anna Papierniak, Anna Barabasz, Maria Kendziorek, Małgorzata Palusińska, Lorraine Elizabeth Williams, Danuta Maria Antosiewicz



PII: S0098-8472(18)31119-5
DOI: <https://doi.org/10.1016/j.envexpbot.2018.09.020>
Reference: EEB 3581

To appear in: *Environmental and Experimental Botany*

Received date: 26-7-2018
Revised date: 21-9-2018
Accepted date: 24-9-2018

Please cite this article as: Kozak K, Papierniak A, Barabasz A, Kendziorek M, Palusińska M, Williams LE, Antosiewicz DM, NtZIP11, a new Zn transporter specifically upregulated in tobacco leaves by toxic Zn level, *Environmental and Experimental Botany* (2018), <https://doi.org/10.1016/j.envexpbot.2018.09.020>

This is a PDF file of an unedited manuscript that has been accepted for publication. As a service to our customers we are providing this early version of the manuscript. The manuscript will undergo copyediting, typesetting, and review of the resulting proof before it is published in its final form. Please note that during the production process errors may be discovered which could affect the content, and all legal disclaimers that apply to the journal pertain.

NtZIP11, a new Zn transporter specifically upregulated in tobacco leaves by toxic Zn level

Katarzyna Kozak^{a,c}, Anna Papierniak^{a,c}, Anna Barabasz^a, Maria Kendziorek^a,
Małgorzata Palusińska^a, Lorraine Elizabeth Williams^b and Danuta Maria Antosiewicz^{a*}

^aUniversity of Warsaw, Faculty of Biology, Institute of Experimental Plant Biology and Biotechnology, Miecznikowa str 1, 02-096 Warszawa, Poland;

^bBiological Sciences, University of Southampton, Life Sciences Building 85, Highfield Campus, Southampton, Hampshire, UK SO17 1BJ

^c KK and AP contributed equally to the paper

* corresponding author: Danuta Maria Antosiewicz

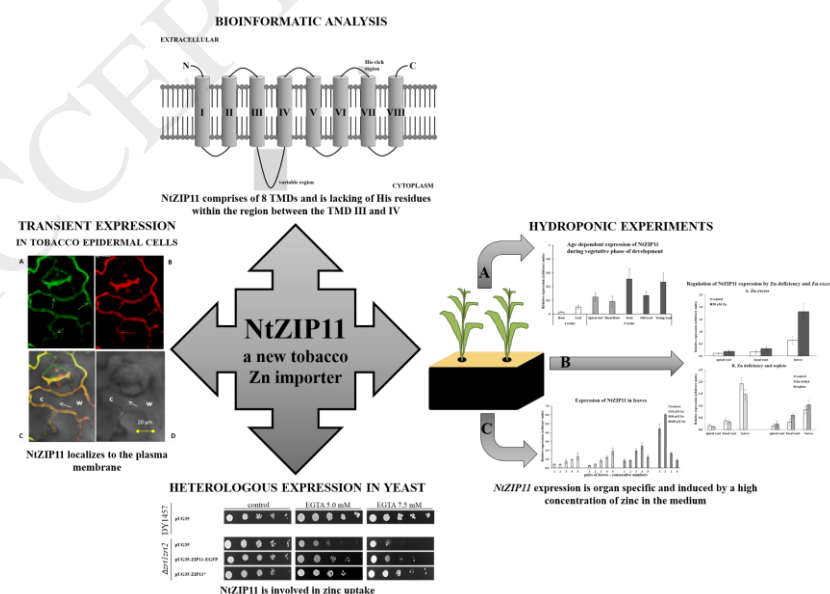
University of Warsaw, Faculty of Biology, Institute of Experimental Plant Biology and Biotechnology, Miecznikowa Street 1, 02-096 Warszawa, Poland

tel: +48-22-5542105; fax: +48-22-5542022;

e-mail: dma@biol.uw.edu.pl

Declarations of interest: none

Graphical abstract



Highlights

- NtZIP11 is a plasma membrane protein mediating Zn uptake, but not Fe, Mn or Cd.
- *NtZIP11* is highly expressed in leaves and upregulated by high Zn concentrations;
- *NtZIP11* is the first known tobacco gene contributing to accumulation of Zn in leaves of tobacco plants at Zn excess;

Abstract

Understanding the molecular mechanisms governing the uptake and accumulation of Zn in the leaves of tobacco plants exposed to high Zn concentrations is important from the perspective of phytoremediation of metal contaminated soil. This study identifies a new candidate gene, *NtZIP11*, which may contribute to Zn accumulation in tobacco leaves. *NtZIP11* encodes a protein of 346 amino acids, with characteristic conserved sequences of the ZIP family of proteins. Phylogenetic analysis shows that NtZIP11 forms a distinct clade with other ZIP11 proteins. Transient expression of GFP-tagged *ZIP11* in the abaxial epidermis of tobacco leaves demonstrates localization at the plasma membrane. Yeast complementation tests and growth assays indicate that NtZIP11 is involved in Zn but not Fe, Mn and Cd uptake. NtZIP11 complements the *zrt1zrt2* mutant deficient in Zn uptake, but not the *fet3fet4* mutant deficient in Fe uptake. Nor does it modify the sensitivity of wild-type yeast, DY1457, to increasing concentrations of Fe, Mn and Cd. *NtZIP11* is expressed in both roots and leaves, with transcript abundance increasing with age. Noteworthy, the expression level of *NtZIP11* is not modulated by Zn-deficiency but is highly upregulated especially in the older leaves by high Zn concentrations (50 and 200 μ M). Our data indicate that the primary role for NtZIP11 is in the uptake of Zn by the cells of tobacco leaves specifically when experiencing high Zn concentrations. It also likely contributes to maintaining a basal supply of Zn to cells at the level of the whole plant. Thus the present study contributes to broadening our understanding of Zn homeostasis mechanisms in tobacco, and clarifying the role of *ZIP11* genes.

Key words: GFP, heavy metals, NtZIP11, yeast growth assay, zinc, ZIPs

1. Introduction

Heavy metals that serve as micronutrients (for example Zn, Ni, Mn, Fe and Cu) function as cofactors in many biological processes (Hall and Williams, 2003; Broadley et al., 2007). Therefore, in plants growing under nutrient-deficient conditions, mechanisms are initiated to cope with and adapt to the stress this can impose (Williams and Salt, 2009; Assunção et al. 2010; Nazri et al. 2017). These include increasing the efficiency of metal uptake from the soil solution, efflux from intracellular stores such as the vacuole, or redistribution of micronutrients from the older organs to support young developing tissues (Sperotto et al. 2014). Plants must also combat toxic effects of elevated heavy metal levels, whether this be micronutrients present in higher than required concentrations or non-essential elements such as Cd, Hg, or Pb that occur as environmental pollutants. Plants have a variety of ways of protecting sensitive cellular metabolic sites from metal excess. These include binding to sites in the cell wall or to chelators within the cytoplasm, regulating metal uptake at the plasma membrane, and sequestration of excess metals in internal stores (primarily vacuoles but also the Golgi) (Williams et al. 2000; Grotz and Guerinot. 2006; Menguer et al. 2013; Ricachenevsky et al., 2015; Vera-Estrella et al., 2017; Farthing et al. 2018). Therefore, metal homeostasis is crucial in maintaining growth and development of plants experiencing metal-related stress. Metal transporters play a vital role, participating in the regulation of uptake, long-distance transport, sequestration and redistribution at the cellular level (Hall and Williams, 2003; Palmgren et al, 2008; Palmer and Guerinot. 2009; Lin and Aarts, 2012; Mikkelsen et al. 2012; Sinclair and Krämer. 2012; Olsen and Palmgren, 2014; Sperotto et al. 2014).

The ZIP (ZRT-, IRT-like proteins) transporters belong to one of the principal metal transport families involved in the regulation of a plant metal homeostasis. This name is based on their sequence similarity to the Zn regulated transporters (ZRT) and Fe regulated transporters (IRT) from yeast. They can transport a variety of heavy metals, primarily Zn but also Fe, Mn, Cu and Cd, depending on the particular transporter. ZIPs are generally found at the plasma membrane but have also been detected at other membranes. Those mediating transport of metal ions into the cytoplasm (either from the apoplast or from cellular organelles) contribute to a tightly controlled system to balance the uptake, utilization and storage of metal ions (Guerinot. 2000; Sinclair and Krämer 2012). In *Arabidopsis* 15 ZIPs have been identified (Grotz and Guerinot 2006) but only a few have been fully characterized. Many of the ZIP genes from different plant species are upregulated by Zn deficiency indicating their

specific role in adapting to the stress of low nutrient availability (López-Millán et al., 2004; Krämer et al., 2007; Chen et al., 2008; Li et al., 2013; Lin and Aarts 2012; Jain et al., 2013; Milner et al., 2013; Nazri et al. 2017). In contrast, *MtZIP6*, *MtZIP7* from *Medicago truncatula* and *OsZIP11* from *Oryza sativa*, showed no induction in Zn-deficient roots and shoots (López-Millán et al., 2004; Chen et al., 2008). Little is known about the involvement of ZIP proteins in the accumulation of Zn in cells from plants exposed to high metal concentrations. *AtZIP6* has been reported to be up-regulated in the roots by Zn excess (Wintz et al. 2003). Thus, there are ZIP transporters that are possibly involved in the accumulation of high amounts of Zn (and other metals) by plants exposed to metal excess, although they have yet to be identified and fully characterized.

Recently, we showed that *NtZIP11-like* from tobacco was upregulated in the leaves of plants exposed to high Zn, suggesting a role in response to Zn-toxicity stress (Papierniak et al., 2018). *ZIP11* genes have not been extensively characterized in any plant species. Most information is available for *Arabidopsis ZIP11*, which was shown to complement the *zrt1zrt2* yeast mutant, but not *fet3fet4*, *smf1* and *ctr1ctr3*. This indicated that Zn, but not Fe, Mn or Cu is a substrate for this protein (Milner et al., 2013). Under control conditions, *AtZIP11* was expressed both in the roots and shoots with the level developmentally regulated. However, regulation by metals, as well as other features, was not examined. Similarly, only some basic information on *OsZIP11* from *Oryza sativa* and *PtZIP11* from *Poncirus trifoliata* are available. *OsZIP11* is expressed in the roots, leaves and panicles, and it was up-regulated by Zn deficiency conditions in the roots of the Zn-efficient genotype IR8192 but not in the Zn-inefficient Erjiufeng (Chen et al., 2008). *PtZIP11*, one of the 14 ZIP genes cloned from *Poncirus trifoliata*, is suggested to be involved in Mn transport and not Zn or Fe as it complemented the *smf1* yeast mutant but not *zrt1zrt2* and *fet3fet4* yeast mutants (Fu et al., 2017).

The focus of this research was on *NtZIP11* from *Nicotiana tabacum*, a new candidate ZIP gene predicted to be involved in the accumulation of high Zn concentrations in tobacco leaves. The aim of the study was to verify this hypothesis by cloning and characterization of *NtZIP11*. Tobacco is known as a plant with a high capacity to accumulate metals including Zn and Cd; therefore, it is a species widely considered to be useful for phytoremediation purposes (Herzig et al., 2003; Doroszewska and Berbeć, 2004; Siemianowski et al., 2011; Herzig et al., 2014;). However, the mechanisms underlying its ability to store metals in leaves remain largely unknown. Molecular understanding of the role of metal transporters in tobacco is

needed as it contributes toward our understanding of metal homeostasis in this species, integral to biotechnological applications such as the generation of plants with increased capacity to accumulate metals.

2. Material and Methods

2.1 Plant material, general growth conditions and hydroponic experiments

Tobacco plants (*Nicotiana tabacum* var. Xanthi) were grown in a growth chamber under the conditions described by Kendziorek et al. (2014). Seeds (after surface sterilization in 8% sodium hypochloride w/v for 2 min) germinated on vertically positioned Petri dishes containing: quarter-strength Knop's medium, 2% sucrose w/v and 1% agar w/v (Barabasz et al. 2010). After three weeks on plates seedlings were transferred to hydroponic conditions on aerated quarter-strength Knop's control medium and cultivated in 2 L pots (5 plants per pot) as described below in detail. The nutrient solution was renewed every 3-4 days unless otherwise indicated. For experiments aimed at examining the response to a range of zinc (Zn) levels, the metal was added as ZnSO₄ to the control medium. In parallel to applied Zn treatments, quarter-strength Knop's medium containing 0.5 μ M Zn was used as a reference (control) medium.

2.1.1 Age-dependent expression of *NtZIP11* during vegetative phase of development

Three-week-old seedlings (three weeks on plates) were grown on liquid control medium for three weeks. Next, they were transferred to 1.2 L pots (2 plants per pot) and grown for subsequent three weeks changing the nutrient solution every 2 days. Plant samples were collected at two developmental stages. *Stage 1*: 4-week old small seedlings (3 weeks on plates and 1 week on hydroponics) whole roots and leaves were collected. *Stage 2*: 9-week old adult plants with formed stem (three weeks on plates and six weeks on hydroponics) younger and older roots and leaves were collected: (a) two young leaves counting from the top (length of the blade of the smallest one was 0.5 cm); (b) two oldest leaves (counting from the base); (c) stem - 3 cm of the middle part; (d) 3-4 cm of the apical region of the root, and 3-4 cm of the basal region of the root (these two sectors were cut out from the roots which grew out directly from the hypocotyl were included, and not from the adventitious roots). The experiment was done in three independent biological replicates. For each repetition samples were collected (material was pooled) from a total of 30 plants (for *Stage 1*), from 10 plants (for *Stage 2*). Collected plant samples were immediately frozen in the liquid nitrogen and stored in -80°C until expression analysis.

2.1.2 Regulation of *NtZIP11* expression by Zn-deficiency and Zn-excess

Three-week old tobacco plants (three weeks on plates) were grown on control medium for 2.5 weeks. To determine if *NtZIP11* expression depends on Zn availability, plants were subsequently subjected to the following Zn regimens: (a) excess Zn for one day (50 μ M); (b) Zn deficit for four days (Zn was not added to the basic medium); (c) resupply of control conditions (for two days) to plants grown at Zn deficit for four days. In parallel plants were grown under control conditions.

Plant material was collected and pooled from a total of 10 plants, immediately frozen in the liquid nitrogen and stored in -80°C till expression analysis. At the end of each experiment, the leaf blades and chosen sectors of the roots were collected. For leaves, the blades of the 2nd and 3rd leaf (counting from the base) without petioles and the major midribs were collected. For roots, 3-4 cm of the apical part, and 3-4 cm of the basal one were collected. Adventitious roots were cut out as they were not included into analysis. The experiment was done in three independent biological replicates.

2.1.3 Expression of *NtZIP11* in leaves

Three-week old tobacco plants (three weeks on plates) were grown on liquid control medium for 2.5 weeks. Afterwards they were transferred to 2 L pots (2 plants per pot) to the medium containing the following Zn concentrations for the consecutive three weeks: 0.5 μ M Zn (control); 10 μ M Zn; 50 μ M Zn and 200 μ M Zn. The nutrient solution was changed every 3-4 days, except that during the last 18 days of exposure the medium was renewed every second day.

The leaves of plants exposed to a range of Zn concentrations were examined for the expression level of *NtZIP11* and for Zn concentration. At the end of treatment, all leaves were removed from the stem. They were collected in groups of two consecutive leaves counting from the base. Each leaf was divided into two halves, and the mid vein was removed. One half was frozen in liquid nitrogen for expression analysis while the second one was dried (55°C , 3 days) for determination of Zn concentration, and material from each pair of leaves was pooled. The experiment was performed in three biological replicates. For each replicate, material for each treatment was collected from 8 plants.

2.2 Cloning of *NtZIP11* and generation of constructs for functional analysis

The full-length sequence of *NtZIP11* was identified on the basis of comparison of the complete genomic sequence of *N. tabacum* available in GenBank under the accession no. AWOK00000000 (Sierro et al., 2013; 2014) with *A. thaliana AtZIP11* cDNAs (query sequence in whole genome shotgun reads in the GenBank database). Several scaffolds of tobacco ZIPs (ZRT, IRT-like proteins) having high homology with the query sequence ($\geq 80\%$) were identified (AWOK01S219909, AWOK01063728, AWOK01217946, AWOK01328322, AWOK01002296). After screening with the FGENESH (Hidden Markov Model) the full putative genomic sequence of *NtZIP11*, including exons, introns, adenylation and transcription start sites, was obtained (AWOK01S219909). On the basis of the results generated by Fgenesh, primers were designed for the amplification of the *NtZIP11* sequence (Table S1).

2.2.1 Generation of the construct for yeast complementation

A full-length sequence of *NtZIP11* was amplified using Phusion HF polymerase (Thermo Scientific) with cDNA transcribed from total RNA isolated from tobacco leaves (as described in section 2.5). Primers were designed to introduce *XbaI* and *BamH* sites (Table S1): *Nt9909_pUG35_for* and *Nt9909_pUG35_rev* and *Nt9909_pUG36_for* and *Nt9909_pUG36_rev*. The PCR product was gel extracted using the Macherey-Nagel PCR clean-up Gel extraction kit (Germany, VWR MANB740609.50), according to the manufacturer's instructions. The *NtZIP11* sequence was ligated into the the *XbaI-BamH* sites of the yeast expression vectors pUG35 and pUG36 (kindly provided by dr M. Migocka, The University of Wrocław, Poland) and confirmed by sequencing. The sequence of the *NtZIP11* cDNA is deposited in the NCBI database (2015) under the accession number XM_016644574.

NtZIP11 was cloned into pUG36 (construct pUG36-EGFP-*NtZIP11*) which attaches a GFP N-terminal to *NtZIP11* and into pUG35 (construct pUG35-*NtZIP11*-EGFP), which attaches GFP C-terminally to *NtZIP11*. Additionally a none-tagged *NtZIP11* was generated (construct pUG35-*NtZIP11*) whereby a STOP codon was present at the end of *NtZIP11* in the pUG35 vector. These vectors contain the methionine260 repressible MET25 promoter (Kurat et al. 2006; Petschnigg et al. 2009).

2.2.2 Generation of the construct for determination of the subcellular localization of *NtZIP11*

Gateway cloning was used to generate a construct for subcellular localization (Curtis and Grossniklaus, 2003). Topo cloning into pENTR™/D-TOPO® (Invitrogen

was carried out using primers to the coding region of *NtZIP11* with a CACC sequence in the forward primer (*Nt9909_pENTR_start* and *Nt9909_pENTR_stop*; Table 1). Subsequently the LR clonase reaction was used to generate *pMDC43-GFP-ZIP11*, which attaches a GFP to the N-terminus of ZIP11. This was sequenced (Genomed, Poland) and used to determine the subcellular localization of the NtZIP11 by transient expression in tobacco leaves (Sparkes et al. 2006).

2.3 Bioinformatic analysis.

The putative protein encoded by *NtZIP11* was predicted. The ORF (open reading frame) of *NtZIP11* was verified by the use of ExPASy (<http://web.expasy.org/translate/>). Alignment of sequences of NtZIP11 and other ZIPs (all sequences were searched in NCBI database with the use of BLAST algorithm) were performed using ClustalW and the phylogenetic trees were constructed with MEGA7.0 software (Tamura et al., 2013) using the maximum likelihood method with 1000 bootstrap replicates. The prediction of membrane-spanning regions and orientation was performed using Phobius software (Käll et al. 2004).

2.4 Isolation of RNA

Plant material stored in -80°C was used for the total RNA extraction. It was performed with the use of an RNeasy Plant Kit (Syngen, #SY341010) according to the manufacturer's recommendations. Obtained samples were digested with DNase I (Invitrogen, #18068015). RNA concentration and purity (the 260/280-nm ratio showed expected values between 1.8 and 2.0) were determined with a Nanodrop spectrophotometer ND 100 (Nanodrop, Willmington, DE, USA) before and after DNA digestion. To confirm the RNA integrity, samples were electrophoresed in 1% agarose gel containing EtBr.

2.5 Determination of the transcript level

Quantitative Real-time PCR (qRT-PCR) was used to determine gene expression. Analysis was performed according to Kendziorek et al (2016) with minor modifications. Briefly, qRT-PCR was conducted in a Roche mastercycler (LightCycler®480 System, Roche) using Light Cycler480 SYBR Green (Master 0488735001) according to the manufacturer's recommendations. As the reference gene/internal control to normalize gene expression and provide quantification the tobacco *NtPP2A* (*protein phosphatase 2A*; AJ007496) gene was used. Its stability in the plant samples collected for expression

analysis was measured and shown in Figure S1. Quantification of the relative transcript levels was performed using the comparative dCt (threshold cycle) method (Livak and Schmittgen, 2001). More detailed description is given in the Supplementary Methods.

2.6 Determination of Zn concentration

Plant samples were dried in an oven at 55°C until constant biomass. Acid digestion was performed in 65% HNO₃ and 39% H₂O₂ (9:1, v:v) in a closed system microwave mineralizer (Milestone Ethos 900, Milestone, Bergamo, Italy). Zn concentrations were determined by flame atomic absorption spectrophotometry (FAAS) (TJA Solution Solar M, Thermo Electron Manufacturer Ltd., Cambridge, Great Britain). Certified reference material (Virginia tobacco leaves CTA-VTL-2; Commission for Trace Analysis of the Committee for Analytical Chemistry PAS and Institute of Nuclear Chemistry and Technology, Warsaw) was included in each analysis run (Barabasz et al., 2012).

2.7 Yeast complementation assay

The constructs pUG35-*NtZIP11-EGFP*, pUG35-*NtZIP11*, pUG36-*EGFP-NtZIP11* (described in subsection 2.2.1) as well as empty vectors pUG35 and pUG36 were transformed into yeast in accordance to the lithium acetate method (Gietz and Schiestl, 2007). In this study three *Saccharomyces cerevisiae* strains were used: (i) the wild-type DY1457 (MATa, *ade1 can1 his3 leu2 trp1 ura3*), (ii) the mutant ZHY3 - *zrt1/zrt2* (DY1457 + *zrt1::LEU2, zrt2::HIS3*) defective in high and low affinity zinc uptake, (iii) the mutant *fet3fet4* (MATa *trp1 ura3 Dfet3::LEU2 Dfet4::HIS3*) defective in high and low affinity iron uptake. Yeast was grown on liquid synthetic complete medium (SC-URA-MET/Glu) containing: yeast nitrogen base supplemented with amino acids (without uracil and methionine) and 2% (w/v) glucose, the pH of the medium was adjusted to 5.3 with 1 M potassium hydroxide (containing 0.2 mM Zn) and incubated overnight at 30°C with shaking. On the next day the OD₆₀₀ was measured (Biophotometer H067, Eppendorf) and adjusted to the approximate value of 0.2. Then, yeasts were grown for another 2-5 hours, OD₆₀₀ was measured again and adjusted to the value 0.2, and series of dilutions were prepared (1.0, 0.1, 0.01, 0.001). 5 µl aliquots of each yeast culture were spotted onto plates containing (SC-URA-MET/Glu) medium solidified with 2% (w/v) agar supplemented with components depending on needs. Yeast growth was monitored for the next 5- 7 days.

2.7.1 Complementation of mutation in Zn uptake

The *zrt1zrt2Δ* yeast strain with the expression of pUG35, pUG35-*NtZIP11*, pUG35-*NtZIP11-EGFP*, pUG36 or pUG36-*EGFP-NtZIP11* as well as WT (DY1457) with the expression of pUG35 or pUG36 (empty vectors) were grown on a SC-URA-MET/Glu medium (containing 0.2 mM Zn) to determine whether Zn is a substrate for the *NtZIP11*. The suspension of yeast cultures were spotted onto the plates containing agar-solidified SC-URA-MET/Glu supplemented with 5.0 and 7.5 mM EGTA (ethylene glycol-bis(β-aminoethyl ether)-N,N,N',N'-tetraacetic acid).

2.7.2 Complementation of mutation in Fe uptake

The *fet3/fet4* yeast strain with the expression of pUG35, pUG35-*NtZIP11*, pUG35-*NtZIP11-EGFP*, pUG36 or pUG36-*EGFP-NtZIP11* as well as WT (DY1457) with the expression of pUG35 or pUG36 (empty vectors) were grown on a plates containing agar-solidified SC-URA-MET/Glu medium containing 50 μM, 100 μM Fe (as FeCl₃).

2.7.3 Sensitivity to Zn, Fe, Mn and Cd

The WT (DY1457) yeast strain with the expression of pUG35, pUG35-*NtZIP11*, pUG35-*NtZIP11-EGFP*, pUG36 or pUG36-*EGFP-NtZIP11* were grown on an agar-solidified SC-URA-MET/Glu medium containing range of concentrations of Zn (2.5 and 5.0 mM Zn as ZnSO₄), Fe (200 μM and 2.5 mM as FeCl₃), Mn (5.0 and 7.5 mM Mn as MnCl₂), or Cd (50 and 75 μM of Cd as CdCl₂). The sensitivity to Zn, Fe, Mn and Cd was monitored.

2.8 Transient expression assay in tobacco epidermal cells

The intracellular localization of *NtZIP11* was determined by monitoring the transient expression of a pMDC43-*GFP-ZIP11* translational fusion product in tobacco epidermal cells after inoculation with *Agrobacterium tumefaciens* GV3101 (C58C1, Rif^R; pMP90, Gm^R) strain carrying the prepared construct. The transient expression was performed according to the protocol by Sparkes et al. (2006) and Siemianowski et al., (2013). More detailed description is given in the Supplementary Methods.

2.9 Statistical analysis.

All presented data are from one experiment that is representative of three to four independent replicate experiments. Statistical significance was evaluated at the 0.05 probability level using Student's t-test. For all experiments, plant samples were collected at the same time of the day (10-12 AM).

3. Results

3.1 Isolation of *NtZIP11* cDNA

The full-length sequence of *NtZIP11* was identified on the basis of comparison of the complete genomic sequence of *N. tabacum* (Sierro et al., 2013; 2014) with *A. thaliana AtZIP11* cDNAs (query sequence in whole genome shotgun reads in the GenBank database). Several scaffolds of tobacco ZIPs (ZRT, IRT-like proteins) with high homology with the query sequence ($\geq 80\%$) were identified (AWOK01S219909, AWOK01S001304, AWOK01S276597, AWOK01S001304, AWOK01S105962). After screening with the Fgenesh (Hidden Markov Model) the full putative genomic sequence of *NtZIP11*, including exons, introns, adenylation and transcription start sites, was obtained. Bioinformatics analysis showed that the genomic sequence consists of 1038 bp with three exons (Figure S2). The deduced amino acid sequence of the NtZIP11 was 346 amino acid long and was predicted to have eight putative transmembrane domains (TMD), and localized outside of the plasma membrane N- and C-terminal tails (longer and very short, respectively) (Figure S3). Between TMD III and IV a hydrophilic region directed toward the inside surface of the membrane was found. This is consistent with known characteristics of ZIP genes (Eng et al., 1998; Guerinot, 2000). The newly identified tobacco homologue of *AtZIP11* was cloned, sequenced, and named *NtZIP11*, according to its similarity to *ZIP11* from *A. thaliana* and other organisms (Figure S3).

3.2 Phylogenetic analysis of NtZIP11

A comparison was performed between the NtZIP11 amino acid sequence and known ZIPs from tobacco, *A. thaliana*, *Vitis vinifera* and two from *Poncirus trifoliata* (PtZIP2 and PtZIP11). For tobacco, all sequences annotated in the NCBI database were taken into consideration. The resulting phylogenetic tree (Figure 1) showed that NtZIP11 formed a distinct clade with other ZIP11 proteins. However, the highest homology was observed between newly cloned NtZIP11 and NsZIP11, NaZIP11, NtomZIP11, which reached 99.7%, 97.4% and 96.5%, respectively (Table S2).

Interestingly, high homology has also been detected between ZIP11 and ZIP2 proteins, which share 66.1-54.4 % identity (Table S2), and these formed a sub-cluster (Figure 1).

The ZIP11 proteins from tobacco, *Arabidopsis*, *P. trifoliata* and *V. vinifera* share sequence conservation. Multiple sequence alignment showed that NtZIP11 does not have histidine residues within the region between the TMD III and IV (Figure S3), which is typical to known ZIP11 proteins. They do not have histidines or have only a few (VvZIP11 has one histidine, PtZIP11 has three). Similarly, ZIP2 proteins also contain only two histidine residues. Thus, except ZIP2 and ZIP11 proteins, the hydrophilic region between spanners III and IV designated the “variable region”, contains a potential metal-binding domain rich in histidine residues (HRD – Histidine Rich Domain). It is present in other ZIP proteins used for alignments. Interestingly, in ZIP11 and also in ZIP2 proteins, there are additional histidine residues within the N-terminal end and in the TM domain VII, which are missing in other ZIPs used for comparison (Figure S3).

3.3 NtZIP11 is a plasma membrane protein

After 3 days from the infiltration of tobacco leaves with the suspension of *A. tumefaciens* containing pMDC-GFP-NtZIP11, the fluorescence of the GFP-ZIP11 fusion protein was observed in the plasma membrane (Figure 2) of the epidermal cells. Due to the fact that the primary cell wall and adjacent plasma membrane are not distinguished by confocal light microscopy, the green signal from the GFP (Figure 2A) and red signal from cell wall stained with the propidium iodide (Figure 2B) overlapped (Figure 2C). Accordingly, the co-localization of the signals derived from GFP and from propidium iodide suggests that NtZIP11 is located in the plasma membrane (Pighin et al., 2014; Siemianowski et al., 2013). The use of tobacco abaxial epidermal cells for transient expression is ideal for discrimination of the localization of a target protein between the plasma membrane and the tonoplast. Cells with irregular shape with several protruding ends contain their central vacuole in the middle part, which do not enter the narrow ends. Around the base of each protruding end there is a region where the tonoplast separates the vacuole from the cytoplasm (Figure 2C white arrow), and can clearly be seen for proteins localising to the tonoplast (Wojas et al. 2009). The lack of GFP-derived signal within this region for NtZIP11 (compare Figure 2C – white arrow with Figure 2A) confirms that this transporter localises to the plasma membrane.

3.4 Heterologous expression of NtZIP11 in yeast

3.4.1 *NtZIP11 is involved in zinc uptake*

To determine whether NtZIP11 transports Zn, a yeast functional complementation assay was performed by using the *zrt1zrt2* yeast double mutant defective in high- and low- affinity Zn-uptake systems. Expression of NtZIP11 (constructs pUG35-*NtZIP11*) significantly improved the defect in yeast growth on low Zn compared with the empty vector control (Figure 3A) suggesting that NtZIP11 transports Zn, likely mediating Zn uptake across the plasma membrane. Interestingly, the presence of the EGFP protein influences the strength of complementation. The expression of *NtZIP11* fused with the EGFP at the N- or C-terminal end (constructs pUG35-*NtZIP11-EGFP* and pUG36-*EGFP-NtZIP11*) reversed the growth of *zrt1zrt2* mutant on low Zn medium more weakly or not at all.

Further to determine the Zn transport ability of NtZIP11, analysis of growth of the wild-type DY1457 strain with and without the expression of all the constructs on media supplemented with high Zn concentrations was performed (Figure 3B). The expression of pUG35-*NtZIP11* rendered the line more sensitive to high Zn, which suggests enhanced uptake of this metal which then caused toxicity.

3.4.2 *NtZIP11-like does not mediate the transport of Fe, Mn and Cd*

To test the ability of NtZIP11 protein to transport Fe, complementation of the *fet3fet4* mutant was analysed. This mutant does not perform as well as wild-type unless supplemented with Fe. The expression of *NtZIP11* (constructs pUG35-*NtZIP11*, pUG35-*NtZIP11-EGFP* and pUG36-*EGFP-NtZIP11*) did not rescue the mutant growth defect on control medium (no added Fe). The growth of *fet3fet4* cells transformed with the empty pUG35/36 vector was similar to the growth of yeast cells transformed with each of the construct containing NtZIP11 (Figure 3C). Moreover, the expression of all constructs in the wild-type DY1457 strain did not render sensitivity to high 200 μ M and 2.4 mM Fe in the medium (Figure 3D). Thus results indicate that the NtZIP11 does not seem to play a role in the transport of Fe.

To examine the ability of NtZIP11 to transport Mn and Cd, the growth of the wild-type DY1457 strain transformed with the pUG35/36 empty vector was compared to wild-type expressing NtZIP11 (pUG35-*NtZIP11*, pUG35-*NtZIP11-EGFP* and pUG36-*EGFP-NtZIP11*) grown at high concentrations of Mn (5.0 and 7.4 mM) and Cd (50 and 75 μ M). As shown in the Figure 3E,F no marked modification of the yeast growth rate was observed suggesting that NtZIP11 is not involved either in Cd nor Mn transport.

3.5 Expression of *NtZIP11* in younger and older plants

To learn about the possible role that *NtZIP11* plays in tobacco, the expression pattern was investigated in selected organs (leaves, roots and stem) of younger and older plants grown at the control conditions (Figure 4). The transcript level was extremely low in young 4-week old seedlings especially in the roots with higher level in the leaves. Expression increased as plants developed with higher levels in 9-week old plants; the highest level was detected in the above-ground parts – in stems and in the leaves. Lower transcript abundance was noted in the roots, and there was little difference in levels in different regions of the root.

3.6 Determination of *NtZIP11* expression in response to low-to-high Zn concentrations.

The relative transcript levels of *NtZIP11* were investigated in plants grown under either Zn excess (50 μM for one day), Zn-deficiency and Zn-replete conditions (two days of control medium followed by four days of Zn deficit). *NtZIP11* expression was significantly upregulated in leaves of plants grown at high 50 μM Zn (Figure 5A). No significant difference was observed in the transcript abundance between the control and experimental plants for all other treatments (Figure 5A,B). The results obtained (Figure 5A) pointed to a specific role of *NtZIP11* in the response of leaves to high Zn. To investigate this further, Zn levels and the expression of *NtZIP11* was determined in leaves of 8.5-week old plants grown for 3 weeks on control medium and on medium supplemented with 10, 50 and 200 μM Zn. Plants exposed to 10 and 50 μM Zn developed similarly to those grown on the control medium (their height was at the similar level and all had 10 leaves); however, the leaves of those exposed to 50 μM Zn were darker green. In the presence of 200 μM Zn, growth was inhibited; plants were smaller and the number of leaves was reduced to 8 (Figure S4).

Under control conditions, the Zn concentration was the highest in the youngest leaves. In the 4th and 5th pair of leaves (closest to the shoot apex) it was 3-fold higher compared to the oldest ones (the 1st and 2nd pair closest to the base of a plant). Such an increase in Zn concentration in the youngest leaves was also detected in plants exposed to the highest Zn levels (200 μM Zn), but not at 10 and 50 μM Zn (Figure 6).

The transcript level of *NtZIP11* in leaves grown on control medium and on medium containing 10 μM Zn was lower in the older leaves (first two pairs of leaves) compared with the younger ones (those close to the shoot apex). The opposite trend was noted as the Zn concentration increased in the medium, and in plants exposed to 200 μM Zn the

highest expression level was found in the oldest leaves (two pair of leaves close to the base of a plant) (Figure 7).

4. Discussion

The role of *ZIP11* genes in plants has not yet been clearly determined. Only a few have been cloned from plants to date and these have not been fully characterized. They include *ZIP11* from *A. thaliana* (Milner et al., 2013), *Vitis vinifera* (Gainza-Cortés et al., 2012) or *Poncirus trifoliata* (Fu et al., 2017). For tobacco, only uncharacterized sequences identified in the NCBI database are available from species such as *N. tabacum*, *N. alata*, *N. plumbaginifolia*; *N. sylvestris*, and *N. tomentosiformis*. This is the first functional characterization of tobacco *NtZIP11*. Sequence analysis of the newly identified and cloned tobacco *NtZIP11* (Figure 1, Figure S3) showed that it contains fundamental characteristics of ZIP family members (Eng, et al., 1998; Guerinot, 2000; Nishida et al., 2008). It encodes a putative transmembrane protein of 346 amino acids (which is within the range of known plant ZIP proteins) consisting of 8 predicted TM domains, a variable hydrophilic (cytoplasmic) region between TMD III-TMD IV, N- and C-terminal ends on the none cytoplasmic side (Figure S3). The consensus sequence within TMD IV of *NtZIP11*, fits the pattern typical for ZIP proteins (VALCFHSVFEGIAIG) (Eng et al., 1998; Guerinot et al., 2000). Moreover, the amino acid sequence is identical in all tobacco ZIP11 proteins, and also in ZIP2 proteins used for comparative analysis. For other ZIPs, the alternative amino acids (indicated in brackets) are present (Figure 1; Figure S3). Phylogenetic analysis shows that there are two closely related sub-branches within the same clade; one with ZIP11 and the second with ZIP2 proteins from different species (Figure 1). The highest homology at the protein level was found between the *NtZIP11*-like and *NsZIP11*, *NaZIP11*, *NtomZIP11* (99.71%, 97.39%, 96.52%, respectively). Identity with *AtZIP11* was lower (66.14%). The level of homology between the *NtZIP11* and ZIP2 proteins used for analysis falls in the range of 63.38 – 54.4 % (Table S2).

Up to now, the TMD IV (with its fully conserved histidyl and glycyl residues) together with the TMD V containing conserved histidine, were proposed to perform the transport function (Eng et al., 1998), and they are present both in ZIP11 and ZIP2 proteins. A conserved histidine is present also in the TMD II of all ZIPs though any role in metal binding/transport is not yet clear. In contrast, ZIP11 and ZIP2 proteins contain an extra histidine in the same position in TMD VII, and in ZIP11 one additional in

TMD VIII (Figure S3). Thus, the role of missing metal transport sequence **HXHXH** in the HRD of the cytoplasmic loop of ZIP11 and ZIP2 proteins might be partially replaced by the presence of histidine in the TMD VII and TMD VIII. The structure of these transport proteins within a membrane is unknown and it cannot be excluded that the role of TMD VII and TMD VIII is not only to anchor the protein but also in the process of metal transfer.

The ZIP proteins, known to mediate transport of several metals including Zn, Mn, Fe, and also non-essential Cd across membranes, have a variety of functions in plants related to the regulation of metal cross-homeostasis (Guerinot, 2000; Lin and Aarts, 2012). Yeast complementation analysis suggests that NtZIP11 localized at the plasma membrane (Figure 2) plays a role in Zn uptake, as it complements the *zrt1zrt2* yeast mutant and confers sensitivity of the DY1457 wild-type to high Zn (Figure 3A,B). Up to now, the only ZIP11 from plants for which the subcellular localization has been established is NtZIP11 (Figure 2). Further analysis determined that it does not transport Fe, Mn or Cd (Figure 3D,F). Similarly, Milner et al. (2013) showed that Zn and not Fe, Mn or Cu is a substrate for ZIP11 from *A. thaliana*, but its membrane localization has not been investigated.

Zn is not only the substrate for NtZIP11, its availability determined its transcript abundance. This was increased by high 50 μM Zn specifically in the leaves (Figure 5A), but not by Zn deficit and resupply conditions (Figure 5B). To learn more about the possible role that NtZIP11 might play in leaves of plants subjected to Zn excess, metal concentration and expression of *NtZIP11* were monitored in leaves of 8.5-week old tobacco plants grown for 3 weeks in the presence of 10, 50 and 200 μM Zn and on the control medium. The Zn concentration in leaves increased with increasing amounts in the medium (Figure 6), however, the upregulation (as compared with the control conditions) of *NtZIP11* was detected at 50 and 200 μM Zn, with the highest (~10 fold) elevation at 200 μM Zn, and only in mature leaves. The expression of *NtZIP11* in the youngest leaves (the pair of leaves closest to the shoot apex) from plants exposed to 50 and 200 μM Zn did not differ from the control ones and from those grown at 10 μM Zn (Figure 7). There are likely two factors closely linked to each other, which contribute to the detected specific expression pattern in tobacco leaves: upregulation by high Zn and the developmental stage of the plant. Our study showed that the *NtZIP11* transcript abundance increased in the roots and in the leaves as a tobacco plant aged; it was lower in 4-week old plants as compared to the 9-week old ones (Figure 4). Therefore, it seems likely that an increase in the transcript level is induced primarily in the older leaves in

which Zn concentration exceeded a threshold over which Zn toxicity might occur, unless Zn detoxification mechanisms are efficient enough to prevent it. Upon mild stress (50 μ M Zn) plants grew relatively well, although metal concentration in examined pairs of leaves was ~10-fold higher compared to 10 μ M Zn grown plants (Figure 6; Figure S4). The height of stems and the number of leaves were the same as in the control plants, but leaves were darker green. In contrast, severe stress (200 μ M Zn) resulted in growth retardation, accompanied with higher Zn concentrations in the leaf blades there was the development of Zn-related necrosis in the lower, older leaves only (Figure S4). From our previous study, it is suggested that the development of necrosis in leaves of plants exposed to high Zn might be a manifestation of a defense mechanism against toxicity of Zn overload (Siemianowski et al., 2013). The excess is loaded into so called “Zn accumulation parenchyma cells”, which with time turn into necrotic regions still keeping Zn inside, protecting neighboring non-accumulating cells from metal toxicity (Siemianowski et al., 2013). It is possible that *NtZIP11* participates in this process and is involved in Zn accumulation specifically in the “Zn-accumulating cells”, which might be related to observed upregulation in lower leaves having necrosis (Figure 7; Figure S4). Upper leaves did not have necrotic regions and, in these, *NtZIP11* expression remained at the control level (Figure 7). Further detailed analysis is required to identify factors involved in the initiation of this process. Noteworthy, *NtZIP11* was first identified while searching for genes involved in accumulation of high Zn in tobacco leaves (Papierniak et al., 2018).

Conclusions. Tobacco is a species used for phytoremediation of metal contaminated soil, including Zn, and leaves are the major organs where metals are stored (Herzig et al., 2003; 2014), however the genes responsible for accumulation of Zn in tobacco leaves had not been identified to date. Specific upregulation of *NtZIP11* detected in the leaves upon exposure to high Zn, but not in the apical and basal parts of roots (Figures 5, 7) suggests a primary role of *NtZIP11* in the uptake of Zn into the cells of mature leaves exposed to Zn excess. Our data also indicate that *NtZIP11* may contribute to maintaining a basal supply of Zn to cells. It was shown that under control conditions there were low stable transcript levels of *NtZIP11* in the roots (both segments – apical and basal), and higher in the above ground parts (stems and leaves) (Figure 4). Similarly, at control conditions, expression of *ZIP11* genes from *A. thaliana*, *V. vinifera* and *P. trifoliata* was also noted both in the roots and in the shoot organs (Gainza et al.,

2012; Milner et al., 2013; Fu et al., 2017). This study has contributed to a greater understanding of Zn homeostasis in tobacco and specifically to the roles of NtZIP11.

Conflict of interest

The authors declare that they have no conflict of interest.

Author contributions

KK and AP designed and carried out all experiments and contributed to the preparation of the manuscript; MK, AB and MP contributed to expression analysis and hydroponic experiments; LEW supervised yeast complementation assays; DMA designed the study concept and experiments, coordinated the research and supervised experiments, performed data analysis and wrote the manuscript. All authors critically revised the manuscript and approved the final version.

Acknowledgements

This work was financially supported by National Science Center, Poland (grant HARMONIA no. NZ3/00527 to DMA). The part of the research on yeast which has been carried out in LEW lab was supported by (BB/L010313/1, and BB/N021150/1).

Appendix A. Supplementary data

Supplementary data include:

Supplementary methods

Table S1: List of primer sequences used in the study.

Table S2: Sequence identity between selected ZIP proteins from *A. thaliana*, *V. vinifera*, *P. trifoliata* and *Nicotiana* species.

Figure S1: RNA transcription levels of *PP2A* gene.

Figure S2: Comparison of introns and exons location within *NtZIP11* and *AtZIP11* genes.

Figure S3: Amino acid alignment of predicted NtZIP11 and ZIP proteins from several species (*Nicotiana*, *Vitis vinifera*, *Poncirus trifoliata* and *Arabidopsis thaliana*) which were used to generate the phylogenetic tree depicted in the Figure 2.

Figure S4: Tobacco plant's response to different Zn concentrations. The arrows indicate necrosis in the leaf blades

References

1. Assunção, A.G.L., Schat, H., and Aarts, M.G.M., 2010. Regulation of the adaptation to zinc deficiency in plants. *Plant Signal. Behav.* 5, 1553-1555.
2. Barabasz, A., Krämer, U., Hanikenne, M., Rudzka, J. and Antosiewicz, D.M., 2010. Metal accumulation in tobacco expressing *Arabidopsis halleri* metal hyperaccumulation gene depends on external supply. *J. Exp. Bot.* 61, 3057-3067.
3. Barabasz, A., Wilkowska, A., Rusczyńska, A., Bulska, E., Hanikenne, M., Czarny, M., Krämer, U. and Antosiewicz, D.M., 2012. Metal response of transgenic tomato plants expressing P1B-ATPase. *Physiol. Plant.* 145, 315-331.
4. Broadley, M.R., White, P.J., Hammond, J.P., Zelko, I. and Lux, A., 2007. Zinc in plants. *New Phytol.* 173, 677-702.
5. Chen, W.R., Feng, Y., Chao, Y.E., 2008. Genomic analysis and expression pattern of *OsZIP1*, *OsZIP3*, and *OsZIP4* in two rice (*Oryza sativa* L.) genotypes with different zinc efficiency. *Russ. J. Plant Physiol.* 55, 400-409.
6. Curtis, M.D. and Grossniklaus, U., 2003. A gateway cloning vector set for highthroughput functional analysis of genes in planta. *Plant Physiol.* 133, 462-469.
7. Doroszewska, T. and Berbeć, A., 2004. Variation for cadmium uptake among *Nicotiana* species. *Genetic Res. Crop Evol.* 51, 323-333.
8. Eng, B.H., Guerinot, D., Eide, M.H., Saier, J., 1998. Sequence analyses and phylogenetic characterization of the ZIP family of metal ion transport proteins. *J. Membrane Biol.* 166, 1-7.
9. Farthing, E.C., Menguer, P.K., Fett, J.P. and Williams, L.E., 2017. OsMTP11 is localised at the Golgi and contributes to Mn tolerance. *Scientific Rep.* 7, 15258.
10. Fu, X-Z., Zhou, X., Xing, F., Ling, L-L., Chun, C-P., Cao, L., Aarts, M.G.M. and Peng, L-Z., 2017. Genome-Wide Identification, Cloning and Functional Analysis of the Zinc/Iron-Regulated Transporter-Like Protein (ZIP) Gene Family in Trifoliolate Orange (*Poncirus trifoliata* L. Raf.). *Front. Plant Sci.* 8, 588.
11. Gainza-Cortés, F., Pérez-Díaz, R., Pérez-Castro, R., Tapia, J., Casaretto, J.A., González, S., Peña-Córtés, H., Ruiz-Lara, S. and González, E., 2012. Characterization of a putative grapevine Zn transporter, VvZIP3, suggests its

- involvement in early reproductive development in *Vitis vinifera* L. BMC Plant Biol. 12, 111.
12. Gietz, D.R. and Schiestl, R.H.. 2007. High-efficiency yeast transformation using the LiAc/SS carrier DNA/PEG method. Nat. Protoc. 3, 31-34.
 13. Grotz, N., Guerinot, M.L., 2006. Molecular aspects of Cu, Fe and Zn homeostasis in plants. Bioch. Biophys. Acta. 763, 595–608.
 14. Guerinot, M.L., 2000. The ZIP family of metal transporters. Bioch. Biophys. Acta. 1465, 190-198.
 15. Hall, J.L. and Williams, L.E. 2003. Transition metal transporters in plants. J. Exp. Bot 54, 2601-2613.
 16. Herzig, R., Guadagnini, M., Rehnert, A., Erismann, K.H., 2003. Phytoextraction efficiency of in vitro-bred tobacco variants using a non-GMO approach. In: Vanek, T., Schwitzguébel, J.P. (Eds.), Phytoremediation Inventory—COST Action 837 View. UOCHB AVCR, Prague, p. 73.
 17. Herzig, R., Nehnevajova, E., Pfistner, C., Schwitzguebel, J-P., Ricci, A. and Keller, C., 2014. Feasibility of labile Zn phytoextraction using enhanced tobacco and sunflower: results of five- and one-year field-scale experiments in Switzerland. Internat J Phytoremed. 16, 735–754.
 18. Jain, A., Sinilal, B., Dhandapani, G., Meagher, R.B., Sahi, S.V., 2013. Effects of deficiency and excess of zinc on morphophysiological traits and spatiotemporal regulation of zinc-responsive genes reveal incidence of cross talk between micro- and macronutrients. Environ. Sci.Technol. 47, 5327–5335.
 19. Käll, L., Krogh, A., Sonnhammer, E.L.L., 2004. A Combined Transmembrane Topology and Signal Peptide Prediction Method. J. Mol. Biol. 338, 1027-1036.
 20. Kendziorek, M., Barabasz, A., Rudzka, J., Tracz, K., Mills, R.F., Williams, L.E. and Antosiewicz, D.M., 2014. Approach to engineer tomato by expression of *AtHMA4* to enhance Zn in the aerial parts. J. Plant Physiol. 171, 1413-1422.
 21. Kendziorek, M., Klimecka, M., Barabasz, A., Borg, S., Rudzka, J., Szczęsny, P., Antosiewicz, D.M., 2016. Engineering high Zn in tomato shoots through expression of *AtHMA4* involves tissue-specific modification of endogenous genes. BMC Genomics 17, 625.
 22. Krämer, U., Talke, I.N., Hanikenne, M., 2007. Transition metal transport. FEBS Lett. 581, 2263-2272.
 23. Kurat, C.F., Natter, K., Petschnigg, J., Wolinski, H., Scheuringer, K., Scholz, H., Zimmermann, R., Leber, R., Zechner, R., Kohlwein, S.D., 2006. Obese yeast:

- triglyceride lipolysis is functionally conserved from mammals to yeast. *J. Biol. Chem.* 281, 491-500.
24. Li, S., Zhou, X., Huang, Y., Zhu, L., Zhang, S., Zhao, Y., Guo, J., Chen, J. and Chen, R., 2013. Identification and characterization of the zinc-regulated transporters, iron-regulated transporter-like protein (ZIP) gene family in maize. *BMC Plant Biol.* 13, 114.
 25. Lin, Y-F. and Aarts, M.G.M., 2012. The molecular mechanism of zinc and cadmium stress response in plants. *Cell. Mol. Life Sci.* 69, 3187–3206.
 26. López-Milán, A-F., Ellis, D.R. and Grusak, M.A., 2004. Identification and characterization of several new members of the ZIP family of metal ion transporters in *Medicago truncatula*. *Plant Mol. Biol.* 54, 583–596.
 27. Menguer, P.K., Farthing, E., Peaston, K.A., Ricachenevsky, F.K., Fett, J.P., Williams, L.E., 2013. Functional analysis of the rice vacuolar zinc transporter OsMTP1. *J. Exp.* 64, 2871-2883.
 28. Milner, M.J., Seamon, J., Craft, E., Kochian, L., 2013. Transport properties of members of the ZIP family in plants and their role in Zn and Mn homeostasis. *J. Exp. Bot.* 64, 369–381.
 29. Milon, B., Wu, Q., Zou, J., Costello, L.C., Franklin, R.B., 2006. Histidine residues in the region between transmembrane domains III and IV of hZip1 are required for zinc transport across the plasma membrane in PC-3 cells. *Bioch. Biophys. Acta.* 1758, 1696–1701.
 30. Nazri, Z.N., Griffin, J.H.C., Peaston, K.A., Alexander-Weber, D.G.A. and Williams, L.E., 2017. F-group bZIPs in barley – a role in Zn deficiency. *Plant Cell Environ.* 40, 2754-2770.
 31. Nishida, S., Mizuno, T., 2008. Obata H. Involvement of histidine-rich domain of ZIP family transporter TjZNT1 in metal ion specificity. *Plant Physiol. Biochem.* 46, 601-606.
 32. Olsen, L.I. and Palmgren, M.G., 2014. Many rivers to cross: the journey of zinc from soil to seed. *Front Plant Sci.* 5, 30.
 33. Palmer, C.M. and Guerinot, M.L., 2009. Facing the challenges of Cu, Fe and Zn homeostasis in plants. *Nature Chem. Biol.* 5, 333-340.
 34. Papierniak, A., Kozak, K., Kendziorek, M., Barabasz, A., Palusińska, M., Tiuryn, J., Paterczyk, B., Williams, L.E. and Antosiewicz, D.M., 2018. Contribution of NtZIP1-Like to the regulation of Zn homeostasis. *Front. Plant Sci.* 9, 185.

35. Petschnigg, J., Wolinski, H., Kolb, D., Zellnig, G., Kurat, C.F., Natter, K., Kohlwein, S.D., 2009. Good fat, essential cellular requirements for triacylglycerol synthesis to maintain membrane homeostasis in yeast. *J. Biol. Chem.* 284, 30981-30993.
36. Pighin, J.A., Zheng, H., Balakshin, L.J., Goodman, I.P., Western, T.L., Jetter, R., Kunst, L., Samuels, A.L., 2014. Plant cuticular lipid export requires an ABC transporter. *Science*. 306, 702-704.
37. Ricachenevsky, F.K., Menguer, P.K., Sperotto, R.A., Fett, J.P., 2015. Got to hide your Zn away: Molecular control of Zn accumulation and biotechnological applications. *Plant Sci.* 236, 1–17.
38. Siemianowski, O., Mills, R.F., Williams, L.E. and Antosiewicz, D.M., 2011. Expression of the P1B-type ATPase *AtHMA4* in tobacco modifies Zn and Cd root to shoot partitioning and metal tolerance. *Plant Biotechnol. J.* 9, 64-74.
39. Siemianowski, O., Barabasz, A., Weremczuk, A., Ruszczyńska, A., Bulska, E., Williams, L.E. and Antosiewicz, D.M., 2013. Development of Zn-related necrosis in tobacco is enhanced by expressing *AtHMA4* and depends on the apoplastic Zn levels. *Plant Cell Environ.* 36, 1093–1104.
40. Sierro, N., Battey, J.N.D., Ouadi, S., Bovet, L., Goepfert, S., Bakaher, N., Peitsch, M.C., Ivanov, N.V., 2013. Reference genomes and transcriptomes of *Nicotiana sylvestris* and *Nicotiana tomentosiformis*. *Genome Biol.* 14, R60.
41. Sierro, N., Battey, J.N.D., Ouadi, S., Bakaher, N., Bovet, L., Willig, A., Goepfert, S., Peitsch, M.C. and Ivanov, N.V., 2014. The tobacco genome sequence and its comparison with those of tomato and potato. *Nature Comm.* 5, 3833.
42. Sinclair, S.A. and Krämer, U., 2012. The zinc homeostasis network of land plants. *Bioch. Biophys. Acta.* 1823:1553-1567.
43. Sperotto, R.A., Ricachenevsky, F.K., Williams, L.E., Vasconcelos, M.W. and Menguer, P.K., 2014. From soil to seed: micronutrient movement into and within the plant. *Front. Plant Sci.* 5, 438.
44. Tamura, K., Stecher, G., Peterson, D., Filipowski, A., Kumar, S., 2013. MEGA6: molecular evolutionary genetics analysis version 6.0. *Mol. Biol. Evol.* 30, 2725-2729.
45. Vera-Estrella, R., Gómez-Méndez, M., Amezcua-Romero, J.C., Barkla, B.J., Rosas-Santiago, P., Pantoja, O., 2017. Cadmium and zinc activate adaptive mechanisms in *Nicotiana tabacum* similar to those observed in metal tolerant plants. *Planta*, 246, 433–451.

46. Williams, L.E., Pittman, J.K., Hall, J.L., 2000. Emerging mechanisms for heavy metal transport in plants. *BBA Biomembranes* 1465, 104-126.
47. Williams, L. and Salt, D.E., 2009. The plant ionome coming into focus. *Curr. Opin. Plant Biol.* 12, 247–249.
48. Wintz, H., Fox, T., Wu, Y-Y., Feng, V., Chen, W., Chang, H-S., Zhu, T., Vulpe, C., 2003. Expression profiles of *Arabidopsis thaliana* in mineral deficiencies reveal novel transporters involved in metal homeostasis. *J. Biol. Chem.* 28, 47644-47653.
49. Wojas, S., Hennig, J., Plaza, S., Geisler, M., Siemianowski, O., Skłodowska, A., Ruszczyńska, A., Bulska, E., Antosiewicz, D.M., 2009. Ectopic expression of *Arabidopsis* ABC transporter MRP7 modifies cadmium root-to-shoot transport and accumulation. *Environ. Pollution.* 157, 2781–2789.

ACCEPTED MANUSCRIPT

Figure legends

Figure 1.

Phylogenetic relationship between NtZIP11 and ZIP proteins from chosen species. (*Nicotiana*, *Arabidopsis thaliana*, *Vitis vinifera* and *Poncirus trifoliata*).

The unrooted tree was constructed based on amino acid sequences identified in the Aramemnon (*Arabidopsis thaliana*), NCBI (*Vitis vinifera*, *Poncirus trifoliata* and *Nicotiana* species) using the MEGA 7.0 software. The lengths of branches are proportional to the degree of divergence. Numbers in the figure represent bootstrap values (1000 replicates). The accession numbers are as follows: *Arabidopsis thaliana* (AtZIP1, AT3G12750; AtZIP2, AT5G59520; AtZIP3, AT2G32270; AtZIP4, AT1G10970; AtZIP5, AT1G05300; AtZIP6, AT2G30080; AtZIP7, AT2G04032; AtZIP8, AT5G45105; AtZIP9, AT4G33020; AtZIP10, AT1G31260; AtZIP11, AT1G55910); *Vitis vinifera* (VvZIP1, XP_002264603; VvZIP3, XP_019078315; VvZIP5, XP_019077951; VvZIP8, XP_002265102; VvZIP11, XP_002265634); *Poncirus trifoliata* (PtZIP2, XP_006488365; PtZIP11, XP_006474910); and *Nicotiana* (*Nicotiana attenuata*: NaZIP1-like, XP_019256554; NaZIP2, OIT06759; NaZIP2-likepred, XP_019233200; NaZIP5, OIT28940; NaZIP5-likepred, XP_019237090; NaZIP10pred, XP_019252985; NaZIP11, XP_019251073; *Nicotiana sylvestris*: NsZIP1-like, XP_009772024; NsZIP2pred, XP_009759327; NsZIP5-likepred, XP_009769157; NsZIP8-likepred, XP_009794548; NsZIP10probable, XP_009772860; NsZIP11, XP_009764644; *Nicotiana tabacum*: NtZIP1, NP_001312674; NtZIP1-like, XP_01646235; NtZIP2-likepred, XP_016473083; NtZIP5-likepred, XP_016449488; NtZIP8-likepred, XP_016458791; NtZIP10probable, XP_016466554; NtZIP11, XP_016500060; *Nicotiana tomentosiformis*: NtomZIP2pred, XP_009607802; NtomZIP5pred, XP_009610335; NtomZIP5-likeX1pred, XP_009597526; NtomZIP10probable, XP_009611861; NtomZIP11, XP_009602718).

Figure 2.

Plasma membrane localization of the NtZIP11-GFP fusion protein transiently expressed in tobacco leaf abaxial epidermis. Confocal images of *NtZIP11-GFP* expressing epidermal cells. Sections were labelled with propidium iodide. (A) GFP fluorescence concentrated to the plasma membrane indicated by green arrows; (B) propidium iodide

staining red of the same cells follows their contours indicated by red arrows; (C) overlapped GFP and propidium iodide signal; (D) bright field. (C,D) white arrows indicate localization of the tonoplast (at the border between the central vacuole (v) and a cytoplasm pushed into a narrow protruding part of a cell (c). Green and red fluorescence is not present in the tonoplast (at the border between a vacuole and a cytoplasm).

Figure 3.

Complementation by *NtZIP11* cDNA of yeast mutants defective in metal uptake on selective media.

Yeast strains used in this study (DY1457, $\Delta zrt1zrt2$ - defective in Zn uptake; $\Delta fet3fet4$ - defective in Fe uptake) were transformed either with the empty vector (pUG35 or pUG36) or with vectors carrying *NtZIP11* with (*) or without a stop codon. Yeast suspension cultures were adjusted to an OD600 of 0.2, and 3 μ l of serial dilutions was spotted on plates containing SC-URA-MET medium supplemented with EGTA (A), ZnSO₄ (B), FeCl₃ (C-D), MnCl₂ (E) and CdCl₂ (F). Zinc concentration in the control medium was equal to 0.2 μ M. The plates were incubated for 3–6 days at 30 °C. The images are representative of three independent experiments.

Figure 4.

Expression of the *NtZIP11* at two developmental stages.

Plants were grown at the control conditions. Expression of *NtZIP11* was determined in 4-week old plants (whole roots and leaves), and in 9-week-old plants (root apex and root base, stem, upper and lower leaves). Transcript level was measured by RT-qPCR and normalized to the *PP2A* expression level. Values correspond to means \pm SD (n=3); Two-fold difference between treatments was considered significant.

Figure 5.

Regulation of the *NtZIP11* expression by Zn availability.

Plants grown at the control conditions for 5.5 weeks were subjected to different Zn regimens: (A) 50 μ M Zn for 1 day; (B) Zn deficit for 4 days (no Zn added to the basic medium), and replete conditions (resupply of control conditions for 2 days to plants grown at Zn deficit for four days). In parallel, plants were grown at the control medium. Expression of *NtZIP11* was determined in the apical and basal parts of the roots. Transcript level was measured by RT-qPCR and normalized to the *PP2A* expression

level. Values correspond to means \pm SD (n=3); Two-fold difference between treatments was considered significant.

Figure 6.

Zinc concentration in tobacco leaves.

Plants grown at control conditions for 5.5 weeks were exposed to the following Zn concentrations: 0.5 μ M Zn (control); 10 μ M Zn; 50 μ M Zn; 200 μ M Zn for 3 weeks. Zn concentration was determined in leaves collected as groups of two consecutive leaves counting from the base: pair 1, pair 2, pair 3, pair 4, pair 5. Values correspond to means \pm SD (n=12); Within each tested Zn concentration, means followed by different letters are significantly different from each other (evaluated by Student's *t* test). ($P \leq 0.05$).

Figure 7.

Expression of the *NtZIP11* in leaves.

Plants grown at the control conditions for 5.5 weeks were exposed to the following Zn concentrations: 0.5 μ M Zn (control); 10 μ M Zn; 50 μ M Zn; 200 μ M Zn for 3 weeks.

Expression of *NtZIP11* was determined in leaves collected as groups of two consecutive leaves counting from the base: 1, 2, 3, 4, 5. Transcript level was measured by RT-qPCR and normalized to the *PP2A* expression level. Values correspond to means \pm SD (n=12); Two-fold difference between treatments was considered significant.

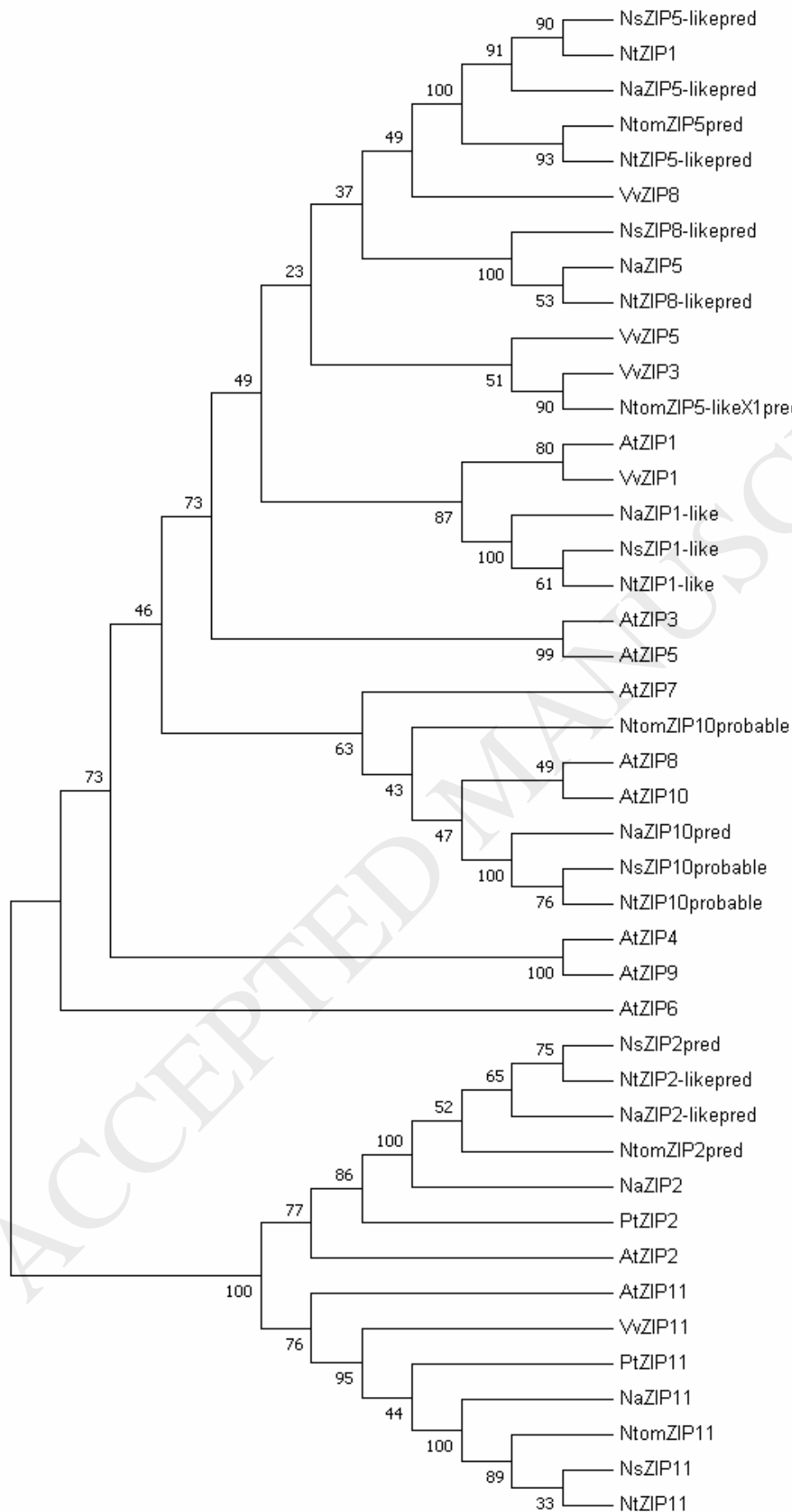


Figure 1

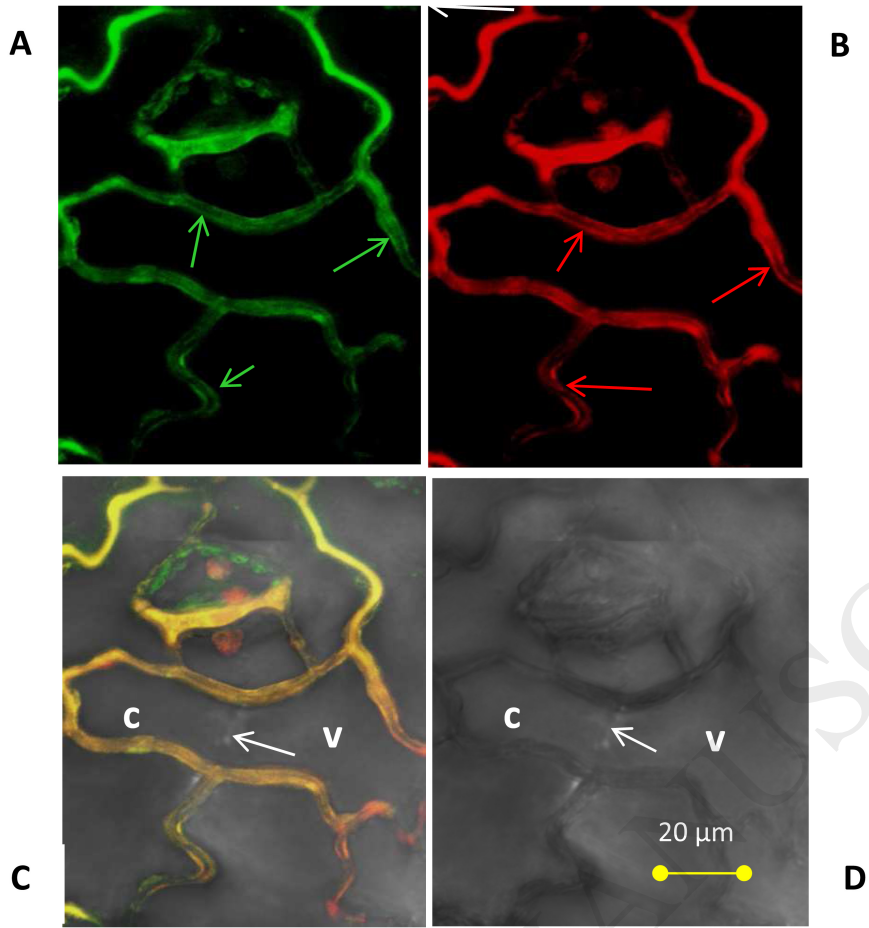


Figure 2

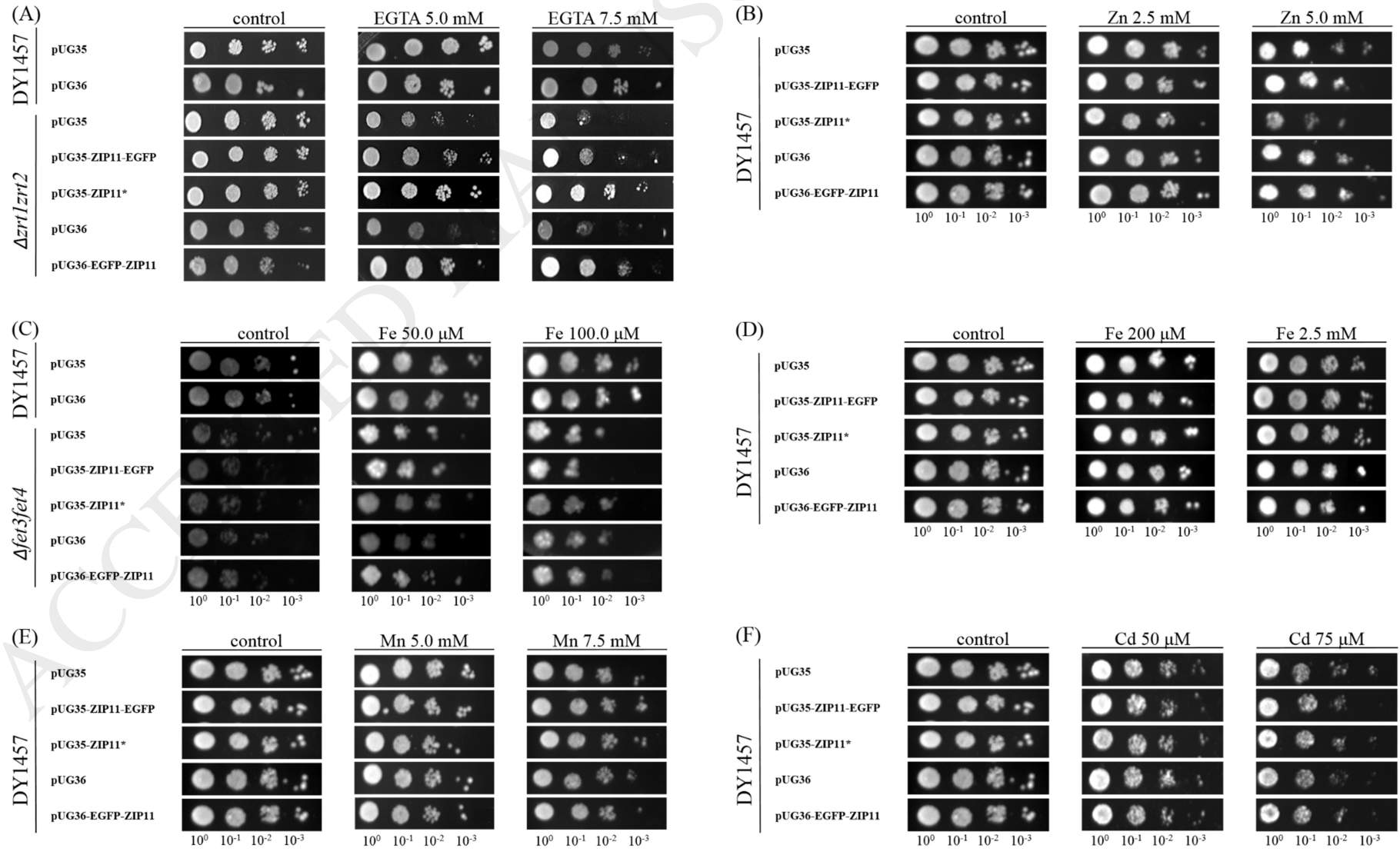


Figure 3

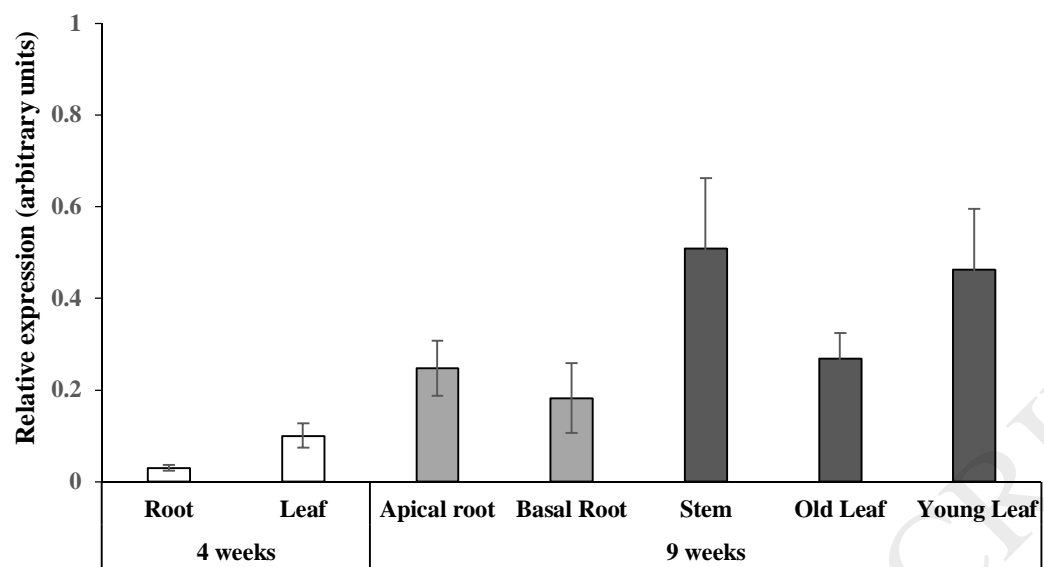


Figure 4

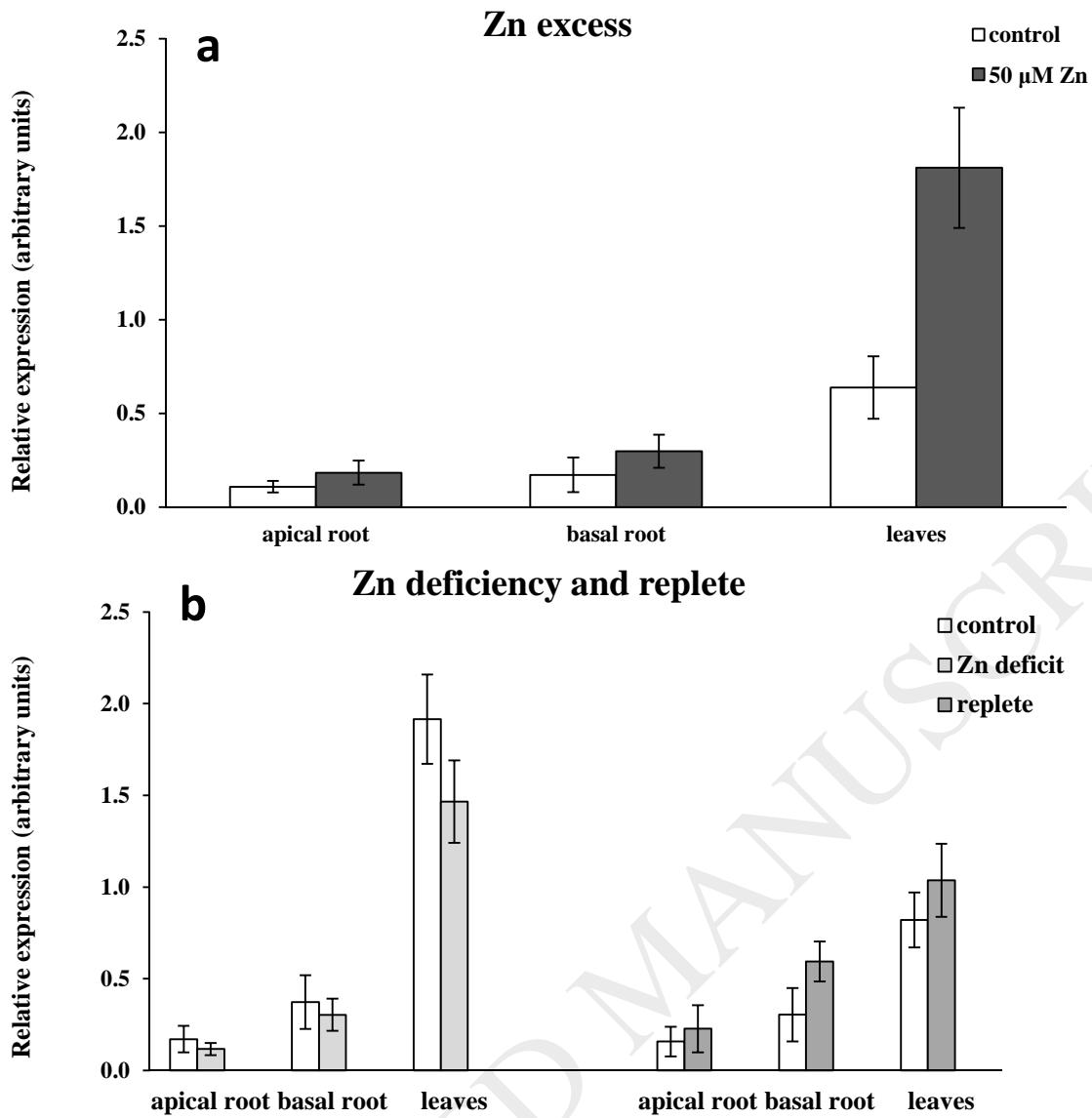
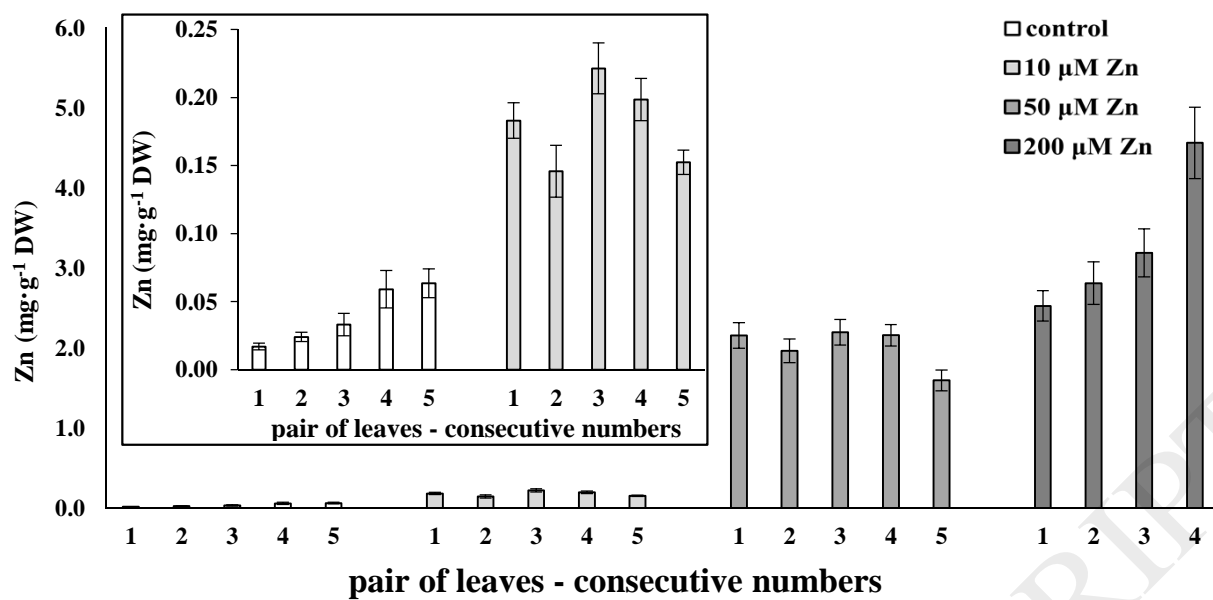


Figure 5



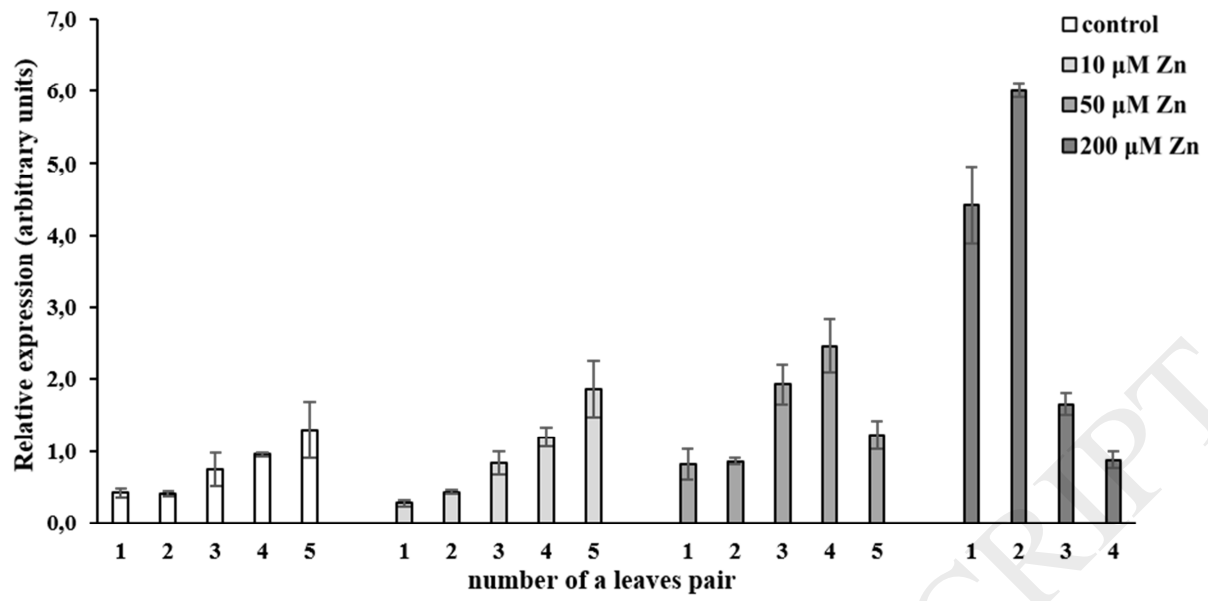


Figure 7